Eur Radiol (2008) 18: 2265–2273
DOI 10.1007/s00330-008-0976-z

MAGNETIC RESONANCE

M. Rasmus
J. Bremerich
T. Egelhof
R. W. Huegli
G. Bongartz
D. Bilecen

Total-body contrast-enhanced MRA on a short, wide-bore 1.5-T system: intra-individual comparison of Gd-BOPTA and Gd-DOTA

Received: 7 August 2007
Revised: 19 March 2008
Accepted: 21 March 2008
Published online: 23 April 2008

Pre-results of the material have been presented at the RSNA, Chicago (2006), Optimization of Contrast-Enhanced Multi-Step Whole-Body MR Angiography with an Open Bore Magnet: Gd-DOTA versus Gd-BOPTA

M. Rasmus (✉) · J. Bremerich · T. Egelhof · R. W. Huegli · G. Bongartz · D. Bilecen
Department of Radiology,
University Hospital Basel,
Petersgraben 4,
4031 Basel, Switzerland
e-mail: mrasmus@uhbs.ch
Tel.: +41-61-2652525
Fax: +41-61-2654354

R. W. Huegli
Department of Radiology,
Kantonsspital Bruderholz,
4101 Bruderholz, Switzerland

Abstract Total-body contrast-enhanced MRA (CE-MRA) provides information of the entire vascular system according to a one-stop-shop approach. Short, wide-bore scanners have not yet been used for total-body CE-MRA, probably due to their restricted field of view in the z-direction. The purpose of this feasibility study is to introduce an image protocol for total-body MRA on a short, wide-bore system. The protocol includes five to six table-moving steps and two injection runs. Two pharmacologically different contrast materials (CM) were applied in ten healthy volunteers in view of possible CM-dependent influences on the protocol outcome (Gd-Bopta, Gd-Dota). Differences consisted of significantly higher CNR with Gd-Bopta with a mean of 73.8±38.7 versus 69.1±34.3 ($p=0.008$), significantly better arterial visualization values with Gd-Dota with a mean of 1.26±0.44 versus 1.53±0.73 ($p=0.003$) and a tendency to less venous overlay with Gd-Dota, mean 1.19±0.44 and 1.34±0.72, respectively ($p=0.065$) (two-tailed Wilcoxon matched-pairs test). Overall 94% of the steps were valued as qualitatively excellent or good. The good results with both CM suggest a transfer to further patient evaluation.

Keywords MR angiography · Gd-Bopta · Gd-Dota · Contrast enhancement · Whole-body angiography

Introduction

Contrast-enhanced MR angiography (CE-MRA) has emerged as a robust, safe and reproducible alternative to digital subtraction angiography for the evaluation of peripheral arterial occlusive disease (PAOD) [1–10].

Total-body 3D contrast-enhanced magnetic-resonance angiography is well suited for the assessment of the peripheral vasculature. In addition, it provides additional data regarding the remaining arterial vessel system [11, 12] according to a one-stop-shop approach. Patients with peripheral arterial disease are frequently found to have additional atherosclerotic lesions in the coronary, renal, and carotid arteries [13]. An impact on patient management in patients with PAOD has been reported [11].

Recently published whole-body CE-MRA data revealed in approximately half of the patients with coronary heart disease at least one additional relevant stenosis in the arterial vasculature including the peripheral, renal and internal carotid artery. This finding underlines the clinical potential of CE-MRA for a certain collectives of patients [8].

Short, wide-bore scanners are intended to provide increased patient comfort due to the shorter length of the scanner and wider gantry diameter (length 125 cm, diameter 70 cm) in comparison to 1.5-T long-bore scanners. The drawback of the short magnet design is accompanied by a field-of-view reduction in z-direction. For total-body MRA, this reduction in spatial extension demands an additional acquisition step to cover the total body. This yields to an extension of acquisition time. Its influence on image quality concerning arterial enhancement, venous overlay and rim artifacts is presently unclear.

The purpose of this feasibility study is to implement a multi-step imaging protocol for total-body MRA on a short, wide-bore system. The imaging protocol consists of five to six automated table steps and two separate intravenous injections. Two contrast media with different pharmacokinetic properties, one with weak albumin binding [14, 15] and one unspecific extracellular substance [16], are applied to evaluate possible pharmacokinetic influences on the protocol outcome. In comparison the weak albumin-binding contrast material is known to tend towards higher and longer vascular peak enhancement [14, 17]

Materials and methods

The study was approved by the local ethics committee; all volunteers gave written informed consent. Ten healthy volunteers (mean age 27.9, 21–41 years; male:female 6:4; mean height 172.7, 160–185 cm; mean weight 70.0 kg, 50–88 kg) were enrolled. All volunteers underwent two total-body CE-MRAs, each with Gd-Bopta (Gadobenate dimeglumine, Multihance®, Bracco Suisse S.A., Mendrisio, Switzerland [14, 15]) and Gd-Dota (Gadoterate meglumine, Dotarem®, Guerbet, Aulnay-sous-Bois, France [16]) in random order with at least 7 days in between. Both contrast materials (CM) correspond to 0.5 mmol/mL gadolinium solution.

MR imaging

All measurements were performed on a Magnetom Espree scanner (1.5 T, Siemens, Erlangen, Germany; bore diameter 70 cm, length 125 cm,) equipped with whole-body array surface coils. A 3D-FLASH (fast low angle shot) sequence with field of view (FOV) 385 mm/step, step width 300 mm, resulting in an overlap of 42.5 mm between all neighboring steps. Acquisition parameters of the two injection protocol are presented in Table 1.

Parallel imaging with GRAPPA algorithm (generalized autocalibrating partially parallel acquisition) was used (GRAPPA-factor 2 for steps *a, e, f* and GRAPPA-factor 3 for *b, c, d*). Higher GRAPPA accelerations, especially in the peripheral steps, were a priory abandoned to prevent expectable consecutively increased signal intensity loss.

The acquisition steps covering supraaortic and calf arteries (steps *a,e*) are acquired with the first contrast injection run, thoracic, abdominopelvic, upper leg and feet arteries (steps *b, c, d, f*) with the second injection (Fig. 1).

The protocol provides double dynamic properties, which means that the last steps of each injection run (*e,f*) might be repeated if dynamic vascular information of the calf and foot arteries are desired. In this setting with healthy volunteers, the last step of the first injection run was exemplarily repeated three times (Fig. 1, Table 1, Fig. 5); a repetition of step *f* was rejected, because no pathologies or delayed vascular enhancement was expected. Both injections were adapted to body weight (BW), (0.3 ml CM × BW)-2 ml and followed by saline flush (30 ml at 2 ml/s; Spectris® MR Injection System, Medrad, Inc, Indianola, Pa; flow rates of each injection; Table 1). The test bolus [18] used for the first run consisted of 2 ml CM followed by saline flush. The care bolus [18] of the second run was followed by subtraction mask acquisition for the second injection steps. Between the first and second injection were a mean of 6.5 min (±2.73) duration. Net acquisition time, including localizer, bolus,

Table 1 Sequence parameters (3D-FLASH) in chronological order: steps *a* and *e* are measured with the first injection's CM, timed by test bolus; the second injection is started depending on the care bolus for the acquisition of steps *b, c, d* and *f*

Injection	Step	FOV read [mm]	FOV phase [%]	Voxel size [mm3]	TR [ms]	TE [ms]	BW [Hz/Px]	TA [s]
Test bolus 2 ml at carotid level, native acquisition for subtraction: e, a								
1st at 2 ml/s	***a***	300	67	1.1×0.8×1.1	4.31	1.39	410	19
	e	385	92	1.0×1.0×1.0	3.54	1.37	510	3×25
Care bolus 2 ml at thoracic level, native acquisition for subtraction: c, d, f, b								
2nd at 50% 2 ml/s 50% 0.7 ml/s	***b***	385	100	1.5×1.0×1.5	3.13	1.15	520	13
	c	385	100	1.6×1.0×1.5	3.12	1.14	520	10
	d	385	100	1.5×1.0×1.5	3.13	1.15	520	10
	f	385	92	1.0×1.0×1.0	3.54	1.37	540	25

Subtraction masks/native datasets for post-acquisition-calculation of subtracted images are taken with equal parameters before step a (a, e), respectively, in between angiographic acquisitions/before step b (b, c, d, f). TA = acquisition time

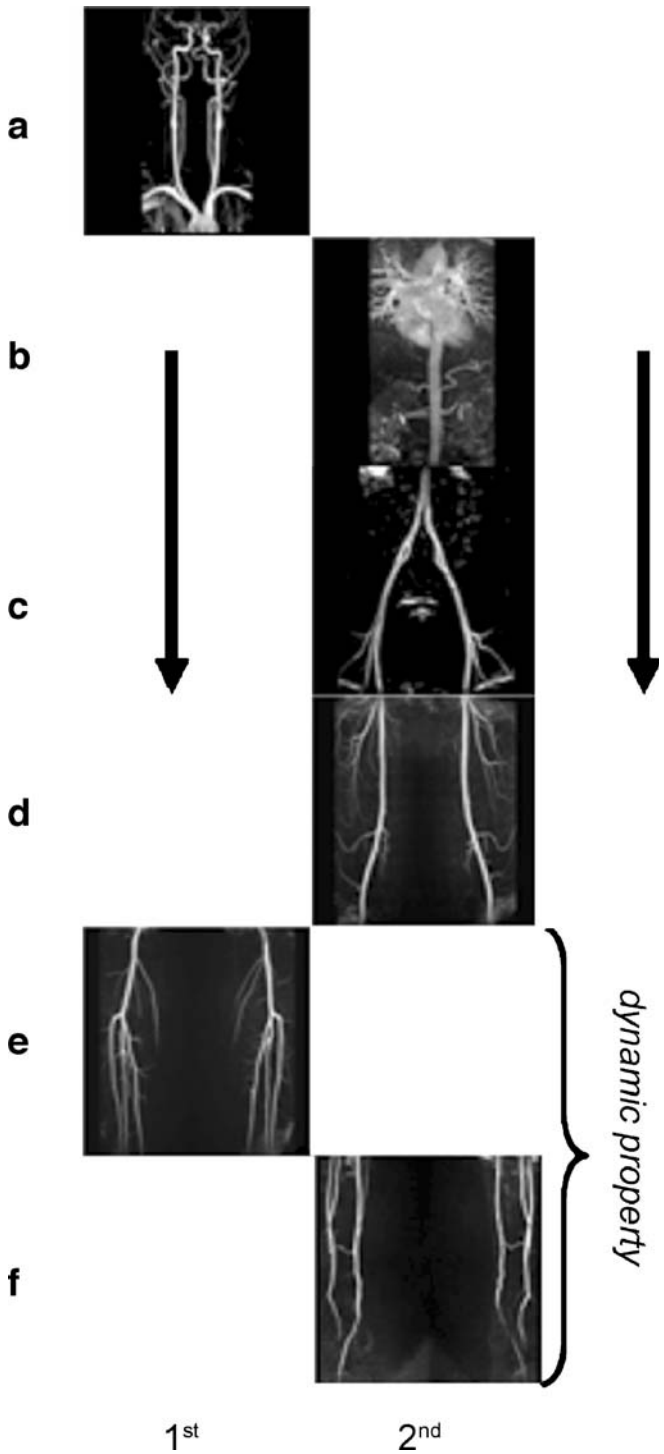

Fig. 1 Injection scheme with first and second injection run, covering in head-foot direction steps *a* and *e*, respectively, *b* to *d* and *f*. The lower steps *e* and *f* can be repeated in view of additional dynamic information (= dynamic property) if dynamic vascular information is desired. In this series of healthy volunteers, limited exemplary dynamic measurements of step *e* (Table 1, Fig. 5) were applied

native and dynamic contrast-enhanced (CE) acquisition times amounted to 11:18 min. Approximated whole examination "in-room" duration was about 40 min.

Qualitative and quantitative evaluation, statistics

The protocols outcome was valuated on the basis of qualitative image analysis. In addition, quantitative analyses were performed to indicate and quantify possible CM-dependent influences. An additional assessment of all data, including all MIP and source image data, was performed in view of exclusion of vascular pathologies.

Qualitative analysis consisted of a blinded consent reading of two experienced radiologists (>10 years of experience) who valued subtracted maximum intensity projection (MIP) images of each step toward venous overlay (VO) and arterial visualization (AV). Both parameters range from I to IV, with

(I) (VO) Excellent, no venous overlay; (AV) excellent arterial visualization
(II) (VO, AV) Fair, observer confident
(III)(VO, AV) Poor, observer not confident
(IV)(VO) Non-diagnostic due to venous overlay; (AV) insufficient arterial contrast.

Quantitative analysis consisted of contrast-to-noise ratio (CNR) measurements of 30 arterial segments (unpaired arterial segments: *basilary artery, thoracic aorta, supra-renal abdominal aorta, infrarenal abdominal aorta*; paired segments: *internal carotid, common carotid, subclavian, renal, common iliac, common femoral, proximal half of superficial femoral, distal half of superficial femoral, popliteal, tibioperoneal trunk, anterior tibial, peroneal, posterior tibial arteries*).

CNR was defined as: $CNR=(SI - SI_{tissue})/Noise$ with SI = mean intra-arterial-ROI signal intensity measured from the source image with best visualization of each arterial segment; SI_{tissue} = mean signal of equal ROI size within adjacent tissue of each segment measured on the same slice as the arterial segment; *noise* = standard deviation of surrounding air's signal measured on one of the source images of each step within the FOV and outside the body within an area of equalized size and position between both CM datasets >50 pixel.

To compare data from the subtracted MIP images and data from the source images, an additional parameter "contrast sum" (CS, CS_mip, respectively) was introduced. Contrast sum was defined as $CS = (SI - SI_{tissue})$ and accordingly for data evaluated from the subtracted MIP images $CS\_mip = (SI\_mip - SI_{tissue\_mip})$.

For statistical analysis the two-tailed Wilcoxon matched-pairs test was used in accordance to the intra-individual comparison setting (SPSS 14.0; indication of significance $p<0.05$).

Results

No vascular pathology was found. No major adverse event occurred [19]. One volunteer suffered temporarily from low blood pressure after Gd-Bopta injection with spontaneous recovery without further medication. The number of table-moving steps was six in eight of ten volunteers; in two the protocol had to be reduced to five steps, as the body length was <170 cm, resulting in n=116 steps, 58 steps with each CM, respectively.

Quantitative analysis

With Gd-Bopta significantly higher mean arterial SI (490 versus 435, p<0.001) and SI_tissue (105 versus 88, p<0.001) resulted, accompanied by higher CNR values. The significant difference of mean CNR amounted to 73.8±38.7 versus 69.1±34.3 (p=0.008) in comparison. CS showed an also significant difference (385 versus 346, p<0.001). CS_mip revealed higher values in comparison to CS for both CM. Between the mean CS_mip values of each CM no significant difference was found (508 versus 518, p=0.12). The difference between mean CS and mean CS_mip (= mean CS - mean CS_mip) amounted to 133 (385–518) within the Gd-Bopta results and 162 (346–508) within the Gd-Dota results. Numeric results are given in Table 2, subdivided for each contrast material for the quantitative parameters' signal intensity (SI), signal intensity of tissue (SI_tissue), contrast-to-noise ratio (CNR), contrast sum (CS) and contrast sum of subtracted MIP images (CS_mip).

Lower contrast-to-noise ratio values were observed in steps *b* and *c* for both CM, in comparison to steps *a, d, e*. Box plots of the stepwise subdivided CNR values are presented in Fig. 2.

Qualitative analysis

Arterial visualization was subdivided into acceptable (I, II) and compromising steps (III, IV); 7 of 116 (6%) steps were valued as of poor or non-diagnostic arterial visualization (III, IV). Compromising AV occurred exclusively in steps of the second run, distributed from thoracic to foot level (Table 3).

The distribution of steps with AV of III or IV revealed one compromising step with Gd-Dota and six with Gd-Bopta with a significant mean difference of 1.26±0.44 versus 1.53±0.73 (p=0.003).

For venous overlay overall also 7 of 116 (6%) compromising steps resulted. Compromising VO occurred mainly in steps *a* and *e* of the first injection run (Table 3). Steps with compromising VO included one compromising step measured with Gd-Dota and six with Gd-Bopta with mean 1.19±0.44 versus 1.34±0.72 (p=0.065) (Table 3).

Discussion

Total-body CE-MRA on a short, wide-bore scanner with a two-injection protocol is feasible. Qualitatively valuable images were acquired for two pharmacologically different contrast materials in an intra-individual comparison in ten healthy volunteers.

In contrast to previous studies performed on long-bore scanners [5, 11, 18, 20, 21], one additional step is needed to compensate the short extension in z-direction.

The acquisition time (Table 1) was between 10 to 25 s/step, net acquisition time 11.18 min, plus duration in between both injections. Complete in-room duration was about 40 min. Acquisition time and approximated achievable in-room durations in a post-experimental setting are comparable to other acquisition schemes [8, 11, 20, 21] with TA per step between of 12 s [11], 13–17 s [20], 19 s [8] or 13–23 s [21], and a reported net acquisition time with two injections of 19:53 min [21] or 40 min for a one injection protocol, but including further examination parts (head, heart) [8] were reported.

A multi-station protocol with two separate contrast media injections [9, 10] was used, as proposed for total-body MRA for conventional scanners [20, 21]. In general,

Table 2 Comparative analysis of quantitative parameters, taken from the whole group of all volunteers and vessel segments (10×30) for each contrast material (two-tailed Wilcoxon matched-pairs test, indication of significance p<0.05)

	SI		SI_tissue		CNR		CS		CS_mip	
	Dota	Bopta	Dota	Bopta	Dota	Bopta	Dota	Bopta	Dota	Bopta
Mean	434.6	489.8	88.4	104.8	69.1	73.8	346.3	385.0	507.8	517.5
Median	371.0	417.0	79.0	95.5	65.4	66.3	280.5	313.5	457.0	464.5
SD	206.4	228.6	40.1	51.8	34.3	38.7	191.0	216.0	265.4	292.9
Min	168.0	174.0	31.0	27.0	13.2	8.5	87.0	75.0	101.0	83.0
Max	1,096.0	1,281.0	262.0	395.0	180.5	217.5	954.0	1,080.0	1,957.0	1,952.0
25%	278.5	315.3	57.0	65.3	42.9	45.8	208.0	228.0	332.3	318.0
75%	556.8	628.3	115.8	136.8	91.8	99.3	461.8	511.8	632.8	633.8
	p<0.001		*p<0.001*		*p=0.008*		*p<0.001*		*p=0.120*	

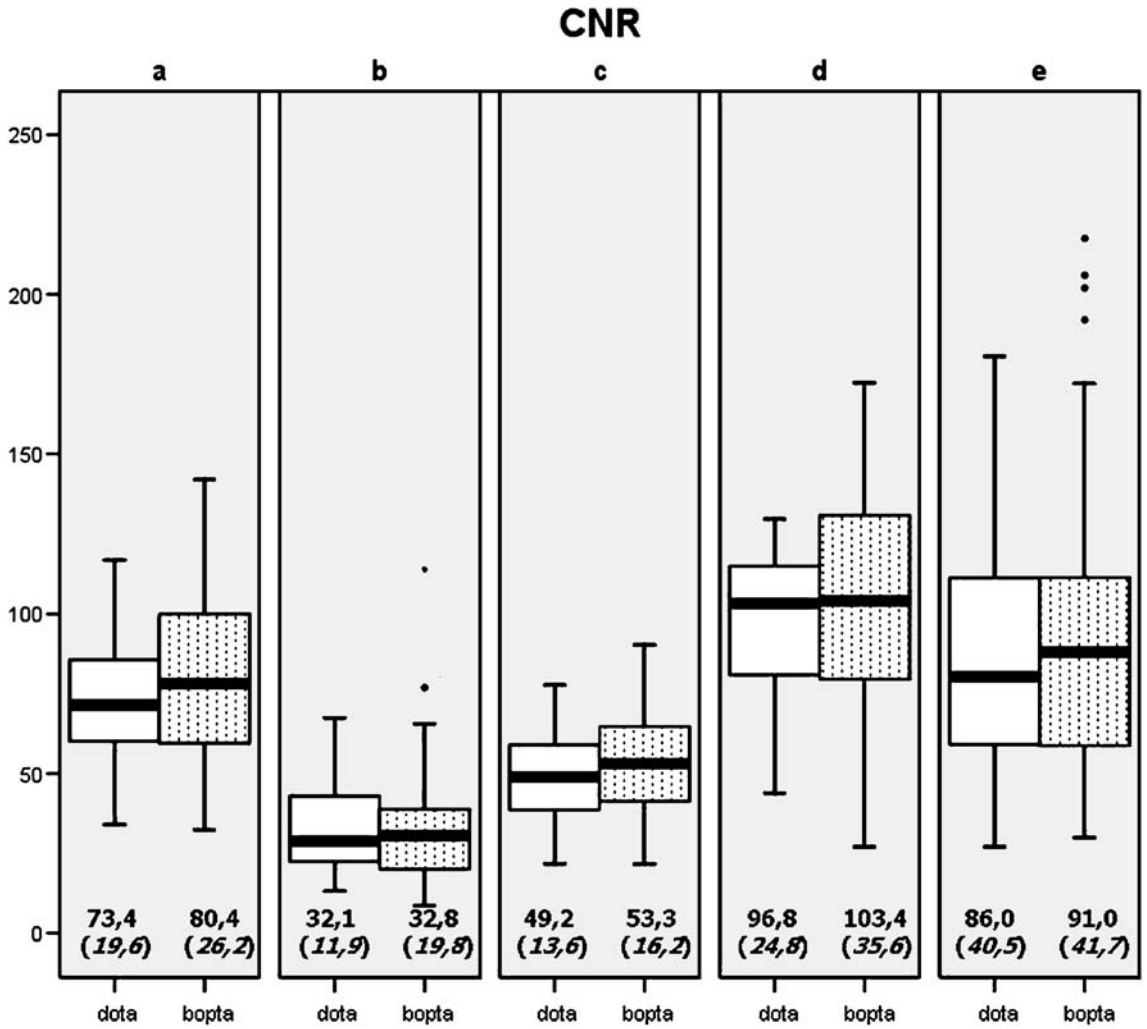

Fig. 2 Box plots of CNR values for Gd-Dota (dota) and Gd-Bopta (bopta), subdivided in steps *a* to *e*. At zero level mean values and SDs are shown; numbers of included vessel segments/step/CM are *a*: 70, *b*: 50, *c*: 54, *d*: 44, *e*: 82

there are at least two advantages of a two injection regime. First, reduction of venous overlay was reported [20]. Secondly, an increase of contrast within supraortal and body segments was found [21]. Both findings might be explained by optimized bolus chasing during the arterial CM passage.

Due to the field inhomogeneity of the static magnetic field, signal loss artifacts at the steps rims occurred. Those

Table 3 Comparative analysis of qualitative parameter arterial visualization (AV) and venous overlay (VO), taken from the whole group of n=58 steps for each contrast material (two-tailed Wilcoxon matched-pairs test, indication of significance $p<0.05$)

	AV		VO	
	Dota	Bopta	Dota	Bopta
I or II	57	52	57	52
III	–	6 (*b,b,c,c,d,f*)	1 *(a)*	5 (*a,a,e,e,f*)
IV	1 (*f*)	–	–	1 (*d*)
Mean	1.26	1.53	1.19	1.34
	p=0.003		p=0.065	

The distribution of given values are grouped into acceptable steps (I and II) and compromising steps with values of III and IV, for which detailed step origin is given in brackets

could be widely reduced by generous overlapping of the adjacent images of 4.25 cm within the composed whole body projections (Figs. 3, 4). Even though duration was in between both injections, a slight venous overlay originating from the first injection was expected for the later steps. Thus, subtraction mask acquisitions for the second injection's steps were positioned in between both injections (Fig. 1, Table 1) to achieve a wide reduction of this possible effect.

Both CM provided good and sufficient arterial visualization. Only few steps were compromised due to insufficient arterial visualization or disturbing venous overlay. Within this limited collective, qualitative results of the protocol with both CM are comparable.

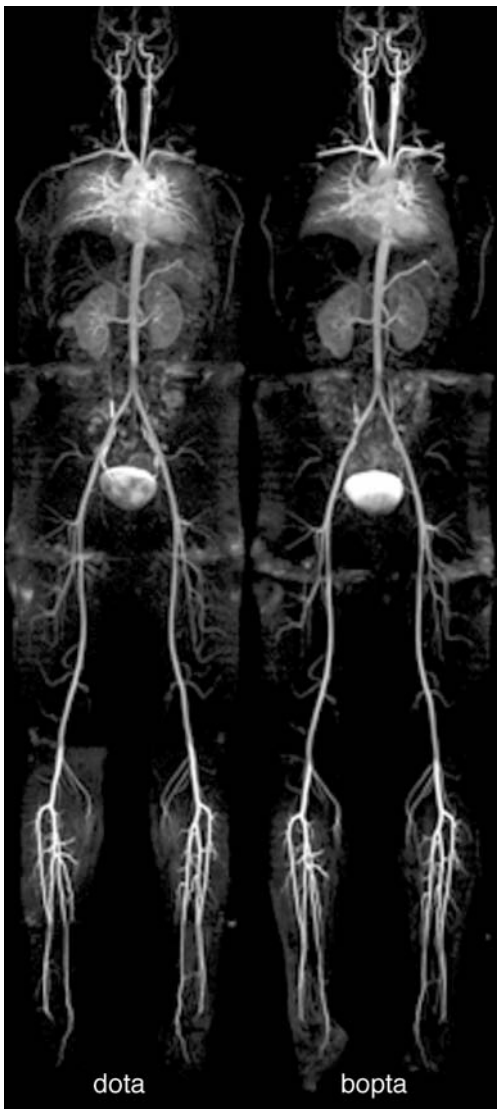

Fig. 3 Example of Gd-Dota (dota) and Gd-Bopta (bopta), composed total-body MRA of one volunteer

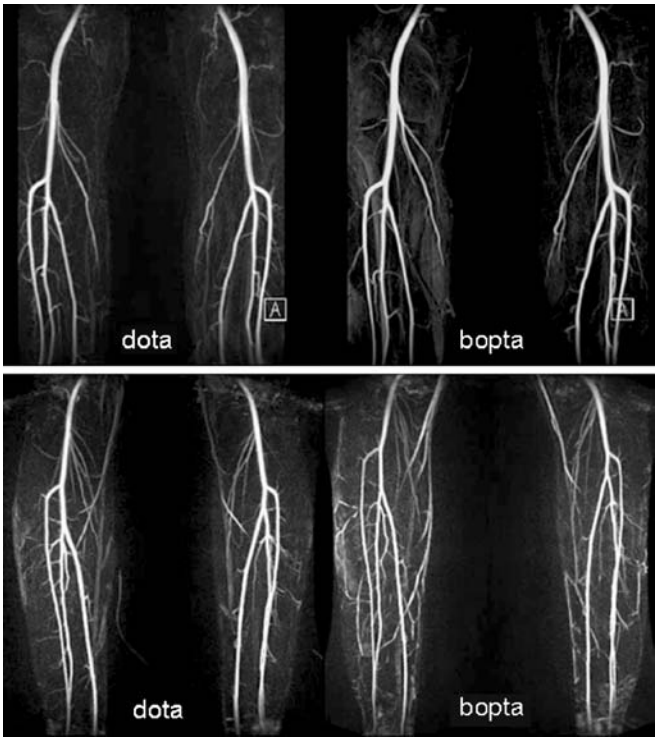

Fig. 4 Intra-individual comparison of lower legs, step *e*. Upper row: Arterial visualization (AV) and venous overlay (VO) of both contrast materials were valued as I = excellent. Lower row: Step *e* of another volunteer with AV = 1 for Gd-Dota, II for Gd-Bopta and VO = II, respectively, III for Gd-Bopta. Artifacts with loss of arterial contrast can be seen at the upper and lower rim in Z direction. Within the total body compositions those effects are widely eliminated by overlapping of 4.25 cm at each rim

An apparent difference between qualitative and quantitative results was found: Significantly higher SI and CNR values resulted for Gd-Bopta (mean CNR difference 74 versus 69, $p=0.008$, Fig. 2), which was also observed in other studies [14, 17, 22]. However, Gd-Dota revealed at least equal image quality with even significantly better arterial visualization-even though with lower SI and CNR values. The reason might be partially explained by the underlying quantification parameter that corresponds closest to the basis of qualitative valuation of arterial visualization: CS_mip, measured from the subtracted MIP reconstructions. Whereas all quantitative parameters measured from the source image data (SI, CNR, CS) resulted in a significant difference, the only quantitative parameter based on the subtracted MIP images did not reveal a significant difference between both CMs. We assume that due to the subtraction process and the voxel selection of MIP reconstruction, the quantitative results of both CMs approximated (that circumstance is also indicated by the comparison between CS and CS_mip of each CM, which revealed a relatively higher difference between CS and CS_mip for Gd-Dota than for Gd-Bopta). Before the background of an insignificant quantitative difference of

the subtracted MIP data, the qualitative AV result seems more congruent. Besides within the qualitative valuation data (range I–IV), the majority of corresponding steps showed equal results ("ties"). Exceptions were mainly presented by the higher number of compromising steps in one group, which mainly led to the significance of difference. Thus, the results indicate, that post-processing procedures do have an influence on the arterial visualization outcome and may somehow soften the effect of underlying quantitative parameter's superiority of source image data (SI, CNR, CS). However, with both CMs the overwhelming number of steps provided acceptable AV results.

The qualitative parameter venous overlay revealed a difference between both CMs with a tendency to more venous overlay with Gd-Bopta within this setting (Table 3). Gd-Bopta is known to have different pharmacokinetics with mild albumin-binding properties with a higher relaxivity and longer vascular peak enhancement. It can be expected-and was also demonstrated in our study-that stronger vascular enhancement leads to higher vessel contrast both in the arterial and venous phase. The influence on image evaluation concerning venous overlay, however, was reported to seem to be of minor importance, as recently demonstrated in peripheral artery disease patients [22]. According to the different measurement protocol used, comparability is limited. In our setting the prolonged vascular enhancement seems to have led to a venous overlay increase in some of the steps, hampering the arterial evaluation. However, the relatively low number of steps with disturbing venous overlay in general in this setting does not allow sufficient statistical proof of causality.

It has to be admitted that in this study with healthy volunteers the focus was on image quality and not valuation of pathologies. In accordance it was desirable to differentiate even slight differences of AV and VO and not to distinguish between diagnostic or nondiagnostic imaging, as pathologies were not even expected.

Thus, the source image data were not included in the qualitative valuation, because the MIP reconstructions concentrate all data concerning VO and AV to one image and thus allow a better differentiating between slight effects than the whole set of source image data can provide.

Both CMs tended towards notably higher CNR values within the peripheral steps compared to central segments

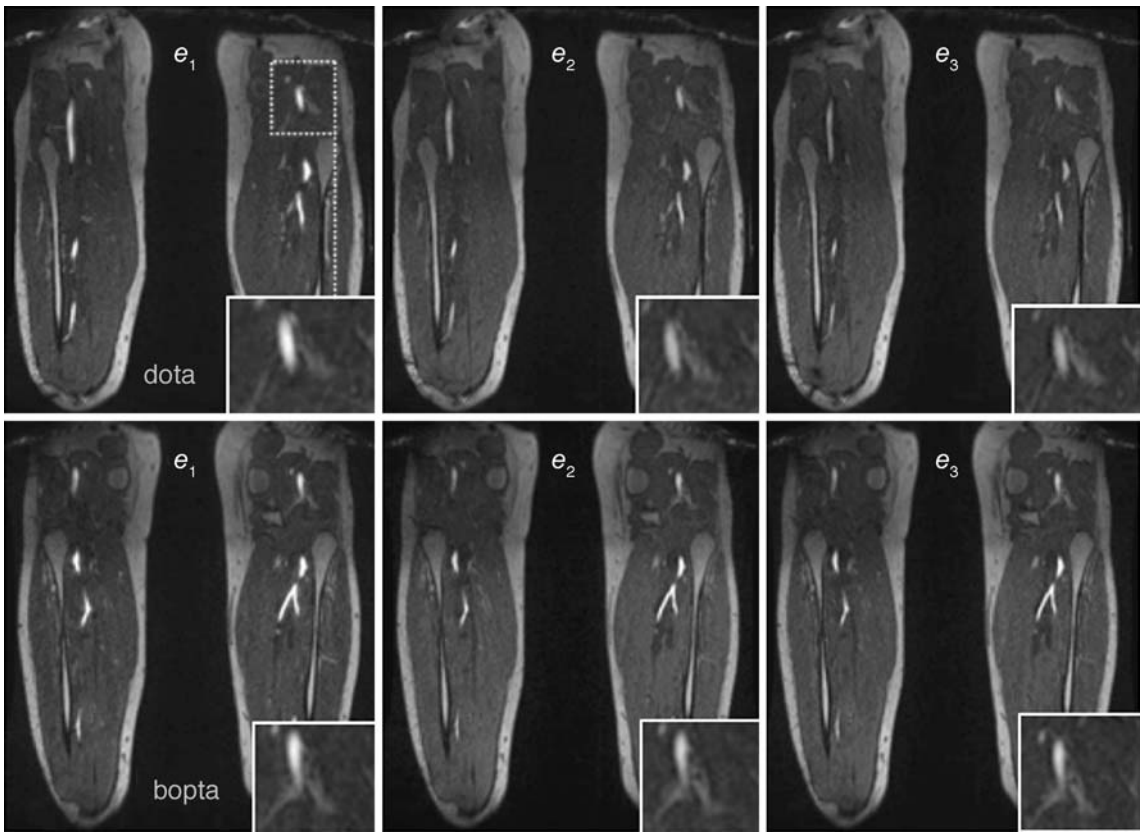

Fig. 5 Source images of step e of both CMs of one volunteer showing the dynamic properties of the protocol. The three repetitions are shown from left to right as e1 = 1st measurement, e2 and e3 = repetitions. A little loss of arterial signal intensity can be seen, as well as a slight increase of venous signal intensity (cut-outs). MIP reconstructions of this volunteer were valued with 1 for AV and VO for both CMs

such as the thoracic and abdominal aorta (Fig. 2). The effect has already been described [22]. The reason for this finding is not completely understood and is likely to be influenced by many factors, such as distribution of CM, surrounding tissues like the lung and intestine and increased coil sensitivity due to less distance to the target region. Besides an increase of GRAPPA acceleration is known to lower SI and depending CNR, which might have influenced this finding, as well as the GRAPPA factor was 3 in the thoracoabdominal steps versus 2 in the peripheral and supraaortic steps. In contrast, the lower resolution in those steps will have diminished the effect, as a lower resolution generally results in higher SI and vice versa.

A major limitation of the study is that the collective of young, healthy and compliant volunteers is highly selective. Potential compromising effects such as lower contrast within the body segments and loss of exactness due to motion and deviation of bolus time, etc., might become somehow more critical in patients and may lead to a reduction of quality. Further evaluation in PAOD patients is necessary to prove the clinical value of total-body CE-MRA using a short, wide bore-system in comparison to established 1.5-T protocol results. Potential modifications for optimized patient evaluations may be on the one hand adaptions of the presented protocol itself, e.g., further reduction of step length to reduce rim artifacts and an increase of overlay or reduction of resolution within the central steps to reduce aquisition time. On the other hand, additional techniques such as calf compression [7, 11, 13, 23–26] or continuous acquisition techniques [27, 28] may provide further improvement for short, wide-bore scanner angiography. It seems likely that with only minor adaptations the protocol will be feasible for clinical practice as an additional option besides established long-bore scanner MRA protocols.

In conclusion, the overall good results with both CM of total-body contrast-enhanced MRA using a short, wide-bore scanner suggest a transfer to further patient evaluation. Gd-Bopta provided better source image SI, whereas the subtracted MIP data sets showed better mean arterial visualization and a tendency to less venous overlay with Gd-Dota within this setting (Fig. 5).

Acknowledgement We thank Tanja Haas and Philipp Madoerin for their great support for MR scanning and image preparation.

References

1. Prince MR, Narasimham DL, Stanley JC et al (1995) Breath-hold gadolinium-enhanced MR angiography of the abdominal aorta and its major branches. Radiology 197:785–792
2. Snidow JJ, Aisen AM, Harris VJ et al (1995) Iliac artery MR angiography: comparison of three-dimensional gadolinium-enhanced and two-dimensional time-of-flight techniques. Radiology 196:371–378
3. Hany TF, Debatin JF, Leung DA, Pfammatter T (1997) Evaluation of the aortoiliac and renal arteries: comparison of breath-hold, contrast-enhanced, three-dimensional MR angiography with conventional catheter angiography. Radiology 204:357–362
4. Rofsky NM, Johnson G, Adelman MA, Rosen RJ, Krinsky GA, Weinreb JC (1997) Peripheral vascular disease evaluated with reduced-dose gadolinium-enhanced MR angiography. Radiology 205:163–169
5. Ruehm SG, Hany TF, Pfammatter T, Schneider E, Ladd M, Debatin JF (2000) Pelvic and lower extremity arterial imaging: diagnostic performance of three-dimensional contrast-enhanced MR angiography. AJR 174:1127–1135
6. Ruehm SG, Goyen M, Barkhausen J et al (2001) Rapid magnetic resonance angiography for detection of atherosclerosis. Lancet 357:1086–1091
7. Vogt FM, Ajaj W, Hunold P et al (2004) Venous compression at high-spatial-resolution three-dimensional MR angiography of peripheral arteries. Radiology 233:913–920
8. Ladd SC, Debatin JF, Stang A et al (2007) Whole-body MR vascular screening detects unsuspected concomitant vascular disease in coronary heart disease patients. Eur Radiol 17:1035–1045
9. Pereles FS, Collins JD, Carr JC et al (2006) Accuracy of stepping-table lower extremity MR angiography with dual-level bolus timing and separate calf acquisition: hybrid peripheral MR angiography. Radiology 240:283–290
10. Meissner OA, Rieger J, Weber C et al (2005) Critical limb ischemia: hybrid MR angiography compared with DSA. Radiology 235:308–318
11. Goyen M, Herborn CU, Kröger K, Ruehm SG, Debatin JF (2006) Total-body 3D magnetic resonance angiography influences the management of patients with peripheral arterial occlusive disease. Eur Radiol 16:685–691
12. Hansen T, Wikström J, Johansson LO, Lind L, Ahlström H (2007) The prevalence and quantification of atherosclerosis in an elderly population assessed by whole-body magnetic resonance angiography. Arterioscler Thromb Vasc Biol 27:649–654
13. Herborn CU, Goyen M, Quick H (2004) Whole-body 3D MR angiography of patients with peripheral arterial occlusive disease. AJR 182:1427–1434
14. Cavagna FM, Maggioni F, Castelli PM et al (1997) Gadolinium chelates with weak binding to serum proteins: a new class of high-efficiency, general purpose contrast agents for magnetic resonance imaging. Invest Radiol 32:780–796
15. Kirchin MA, Pirovano GP, Spinazzi A (1998) Gadobenate dimeglumine (Gd-BOPTA). An overview. Invest Radiol 33:798–809

16. Magerstadt M, Gansow OA, Brechbiel MW et al (1986) Gd(DOTA): an alternative to Gd(DTPA) as a T1, 2 relaxation agent for NMR imaging or spectroscopy. Magn Reson Med 3:808–812
17. Rohrer M, Bauer H, Mintorovitch J, Requardt M, Weinmann HJ (2005) Comparison of magnetic properties of MRI contrast media solutions at different magnetic field strengths. Invest Radiol 40:715–724
18. Meaney JF (2003) Magnetic resonance angiography of the peripheral arteries: current status. Eur Radiol 13:836–852
19. Patel N, Sacks D, Patel RI et al (2003) Society of interventional radiology technology assessment committee. SIR reporting standards for the treatment of acute limb ischemia with use of transluminal removal of arterial thrombus. J Vasc Interv Radiol 14:453–465
20. Fenchel M, Requardt M, Tomaschko K et al (2005) Whole-body MR angiography using a novel 32-receiving-channel MR system with surface coil technology: first clinical experience. J Magn Reson Imaging 21:596–603
21. Klessen C, Asbach P, Hein PA et al (2006) [Whole-body MR angiography: comparison of two protocols for contrast media injection]. Rofo 178:484–490
22. Wyttenbach R, Gianella S, Alerci M, Braghetti A, Cozzi L, Gallino A (2003) Prospective blinded evaluation of Gd-Dota- versus Gd-Bopta-enhanced peripheral MR angiography, as compared with digital subtraction angiography. Radiology 227:261–269
23. Bilecen D, Aschwanden M, Heidecker HG, Bongartz G (2004) Optimized assessment of hand vascularization on contrast-enhanced MR angiography with a subsystolic continuous compression technique. AJR 182:180–182
24. Herborn CU, Ajaj W, Goyen M, Massing S, Ruehm SG, Debatin JF (2004) Peripheral vasculature: whole-body MR angiography with midfemo ral venous compression—initial experience. Radiology 230:872–878
25. Gluecker TM, Bongartz G, Ledermann HP, Bilecen D (2006) MR angiography of the hand with subsystolic cuff-compression optimization of injection parameters. AJR 187:905–910
26. Bilecen D, Jager KA, Aschwanden M, Heidecker HG, Schulte AC, Bongartz G (2004) Cuff-compression of the proximal calf to reduce venous contamination in contrast-enhanced stepping-table magnetic Resonance angiography. Acta Radiol 45:510–515
27. Vogt FM, Zenge MO, Ladd ME et al (2007) Peripheral vascular disease: comparison of continuous MR angiography and conventional MR angiography-pilot study. Radiology 243:229–238
28. Kruger DG, Riederer SJ, Grimm RC, Rossman PJ (2002) Continuously moving table data acquisition method for long FOV contrast-enhanced MRA and whole-body MRI. Magn Reson Med 47:224–231